Catalysis Letters Vol. 102, Nos. 1–2, July 2005 (© 2005)
DOI: 10.1007/s10562-005-5195-5

In situ nanoscale wet imaging of the heterogeneous catalyzation of nitriles in a solution phase: novel hydrogenation chemistry through nanocatalysts on nanosupports

Pratibha L. Gai[a,b,*], K. Kourtakis[a], and E.D. Boyes[a]

[a]*Central Research and Development, Experimental Station, DuPont, Wilmington, DE, 19880-0356, U.S.A*
[b]*Department of Materials Science, University of Delaware, Newark, DE, U.S.A*

Received 9 December 2004; accepted 2 March 2005

Wet-environmental transmission electron microscopy studies of heterogeneous hydrogenation of complex nitriles in a liquid phase over new mesoporous cobalt-promoted ruthenium nanocatalysts on reducible nanotitania supports are presented. The desorbed organic products in the dynamic liquid phase hydrogenation are imaged *situ* on the nanoscale. The direct studies on the ''nanocomposite'' catalysts are correlated with parallel reaction chemistry measurements. They demonstrate high hydrogenation activity at low operating temperatures in the presence of atomic scale anion vacancy defects associated with Lewis acid sites at the nanosupport surface and an electronic and synergistic contribution to the promoter mechanism. The combined synergistic effect between the two metals and the interaction with the reduced nanosupport leading to an electronic modification lead to highly reactive site for the hydrogenation catalysis. The results illustrate novel selective hydrogenation chemistry with mesoporous nanocatalyst systems on nanosupports.

KEY WORDS: hydrogenation; nitriles in solution phase; wet *in situ* imaging; nanocatalysts.

1. Introduction

Technological processes for the hydrogenation and polymerization of complex organic molecules are often derived from solutions using heterogeneous catalysts and the associated dynamic chemical reactions occur on the nano (molecular) scale. Hydrogenation of adiponitrile (ADN, $NC(CH_2)_4CN$) in a liquid medium (phase) is used in the chemical industry to produce hexamethylene diamine (HMD, $H_2N(CH_2)_6NH_2$) and has received considerable attention [1–4]. Alkylated amines are key organic intermediates in the manufacture of polyamides for fiber and mechanical industries [2,4]. Currently, the hydrogenation of ADN to HMD is carried out with the dinitrile in a solvent such as methanol under gaseous hydrogen over Raney nickel (or cobalt) formed by Ni–Al alloy, from which Al is dissolved in alkaline solution leaving a hydrogenated surface [l–4]. However, the recovery of the fragile catalysts can be difficult and residual amounts of Al can have a deleterious effect on the catalyst selectivity [1,2]. The hydrogenation of nitriles using noble metals on MgO and on carbon have not addressed the catalyst reactivity for HMD and the role of microstructure [5,6].

The dynamical molecular level reactions between organic molecular solutions and inorganic surfaces critically influence functions of solution-based heterogeneous catalysis for hydrogenation and polymerization technologies and molecular electronics. The activity and selectivity of catalysts in the hydrogenation of ADN in a liquid phase to HMD depends critically on the catalyst microstructure under operating conditions. The existing understanding of the solution-based reactions in catalytic hydrogenation and subsequent polymerization is based on static, room temperature post-reaction *ex situ* studies of dry products. Since organic molecular solutions can change structure/morphology upon drying, this has hindered the design of new active catalysts. Furthermore, nanostructural modifications during the liquid hydrogenation and the causes of the catalyst deactivation, e.g. due to catalyst spreading on the substrate [7], metal–substrate interactions [8–10], substrate particle size and promoter effects are not well understood. We have carried out *in situ* wet -electron microscopy studies in liquid environments of the hydrogenation of ADN in a liquid phase over novel nanocatalysts of ruthenium and transition metal and noble metal promoted Ru on nano-titania and on other nano-substrates at operating temperatures to develop highly active catalyst surfaces for low temperature heterogeneous hydrogenation routes for HMD.

2. Experimental

2.1. Catalyst materials

We prepared nanocatalysts of Ru (5 wt%) incorporated into reducible rutile nanotitania (Ru/TiO_2), Ru

* To whom correspondence should be addressed.
E-mail: pratibha.l.gai@usa.dupont.com

with cobalt promoters on titania (by wt% $Ru_{0.05}$ $Co_{0.1}$ $Ti_{0.85}$ oxide, ($Co–Ru/TiO_2$), and with Au promoters ($Ru_{0.05}$ $Au_{0.025}$ $Ti_{0.925}$ oxide), using a single-step sol–gel process [11–13]. Group VIII metals such as Ru are important hydrogenation catalysts. We used soluble metal components of Ru-chloride, Co-chloride and tetrachloroauric acid ($HAuCl_4$), added as aqueous solutions to titanium n-butoxide, as described below.

In the sol–gel process used in our synthesis of novel nanocatalysts, water and any aqueous solution are added in a drop-wise fashion to the alcohol-soluble alkoxide and other reagents to induce hydrolysis and condensation reaction. A molar ratio of water:alkoxide 4:1 was used and the H_2O: alkoxide stoichiometry was controlled so that complete hydrolysis of titanium *n*-butoxide was achieved. Synthesis procedures are as follows:

For dried gel (xerogel) nanocatalyst preparation of $Co_{0.1}$ $Ru_{0.05}$ $Ti_{0.85}$ oxide: in an inert atmosphere-drybox, titanium *n*-butoxide (115.72 g) was added to ethanol (240 mL) along with a 1 M $CoCl_2$ (39.806 mL) in ethanol solution. This mixture was loaded into a 1 L resin kettle. In a dropping funnel, H_2O (25.50 mL) was combined with ruthenium trichloride (4.508 g) and ethanol (240 mL). This aqueous solution was slowly added to the alkoxide solution. The entire assembly was under nitrogen purge during this addition. A gel point was rapidly realized. The material was dark brown in color, was aged for 3 days and dried under vacuum at 120 °C for 5 h.

For dried gel of Ru(0.05)/Ti oxide: In an inert atmosphere-drybox Ti-*n*-butoxide (118.044 mL) was combined with ethanol (78.696 mL) and loaded into a 1 L kettle. Additional ethanol was added to this solution. In a separate container, $RuCl_3$ (4.205 g) was combined with water (56.35 mL) and loaded into a dropping funnel, along with ethanol (196.1325 mL). Under a nitrogen purge, the aqueous solutions were slowly added to the alkoxide solution. A gel point was rapidly realized. The material was aged for 3 days before drying at 120 °C under vacuum for 5 h. For dried gel of $Ru_{0.05}$ $Au_{0.025}$ /$Ti_{(0.925)}$ oxide: the same procedure was used, except that 32.49 mL of a 0.26871 M $HAuCl_4$ solution in water was added to the aqueous $RuCl_3$ solution.

For comparison, we also prepared the nanocatalysts on different supports, including alumina. Metal catalysts on titania showed higher reactivity.

2.2. Pore volume distributions and BET surface areas

Dinitrogen adsorption/desorption measurements were performed at 77.3 K, on Micromeritics [14] ASAP® model 2400/2405 porosimeters. Samples were degassed at 150 °C, overnight prior to data collection. Surface area measurements utilized a 5-point adsorption isotherm collected over 0.05–0.20 p/p_0 and analyzed via the well-known BET method [15]. Pore volume distributions utilized a 27-point desorption isotherm and were analyzed via the BJH method [16].

2.3. In situ environmental transmission electron microscopy (ETEM) under liquid environments

We used an *in situ* atomic resolution environmental-transmission electron microscope (ETEM) pioneered by Gai *et al.* [17–19] which is integrated with a microreactor (environmental cell-ECELL) inside the ETEM, for monitoring thehydrogenation of liquid nitriles in real-time. A conventional reactor type gas-manifold system enables inlet of gases into the ECELL of the ETEM and a mass spectrometer enables the identification of reactants and products. High gas pressures up to 1 atm and temperatures of up to 1000 °C are possible in the ECELL, however lower gas pressures (a few torr) are used for atomic-scale resolution. This is because at higher gas pressures some loss of resolution is possible due to multiple scattering and absorption of electrons through thicker gas layers. (The ETEM design [18,19] has been adopted by commercial TEM manufacturers). Low-dose electron beam imaging is used to prevent any beam damage to the sample and calibration experiments are carried out without the beam (with the beam switched on for a few seconds only to record the final state of the reaction), to confirm *in situ* data. A video imaging system connected to the ETEM facilitates recording of dynamic events in real-time. Time and temperature resolved studies are possible. Under liquid environments, image contrast was blurred and attempts were made to observe similar areas before and during reactions.

High precision nanocatalyst compositions were obtained using energy dispersve X-ray spectroscopy (EDX) in a FEI Tecnai FE(S)TEM at 200 keV.

For ETEM in liquid environments (hereafter referred to as wet-ETEM), a liquid feed sample holder enabling controlled injection of nanoliters to microliters of liquids and with heating capabilities was employed [20,21], and hydrogen gas was inserted utilizing the gas-manifold of the ETEM [18]. This procedure enabled us to directly observe reactions between the ADN liquid, hydrogen gas and the catalyst at operating temperatures. Changes at the catalyst surface and desorbed products were observed by selected area electron diffraction (SAED) and real-space imaging at the nanoscale. Energy dispersive X-ray (EDX) spectroscopy, with electron nanoprobes was used to obtain nanocatalyst compositions. Samples in the liquid environment were electron-beam sensitive and experimental conditions and imaging procedures with very low dose electrons, similar to those used for beam sensitive zeolites [21] and for liquid environments [22–24] were employed. Calibration experiments were performed to confirm *in situ* studies [18,21]. Desorbed products were analyzed using a

matrix-assisted laser desorption / ionization (MALDI) mass spectrometer (MS) which is capable of analyzing very small quantities (pg) of materials [25]. We also carried out parallel catalyst reactivity tests to correlate with the in *situ* studies.

2.4. Parallel reactivity tests

To confirm *situ* ETEM studies, parallel hydrogenation reactivity tests on the catalysts were performed using 10 wt% solution of methanol containing 0.75% (wt) of NaOH in shaker tubes at ~100 °C and under flowing hydrogen and after the reaction, the products were analyzed by gas chromatography.

3. Results and discussion

N_2 pore volume and size distributions are presented in Figure 1a and b, and show BET surface areas of ~86 m^2/g and single point pore volume of 0.197 cc/g. No evidence for microporosity (pores <2 nanometers (nm)) was observed; pores were generally mesoporous, with an average pore diameter of about 5 – 6 nm. Rutile TiO_2 is tetragonal with lattice parameters of, $a = 0.46$ nm and $c = 0.296$ nm. Ru is hexagonal with $a = 0.27$ nm and $c = 0.428$ nm and Co is in the form of FCC, with $a = 0.3545$ nm.

Freshly prepared nanosized catalysts on the surface of crystalline nanotitania (rutile) particles of a few tens of

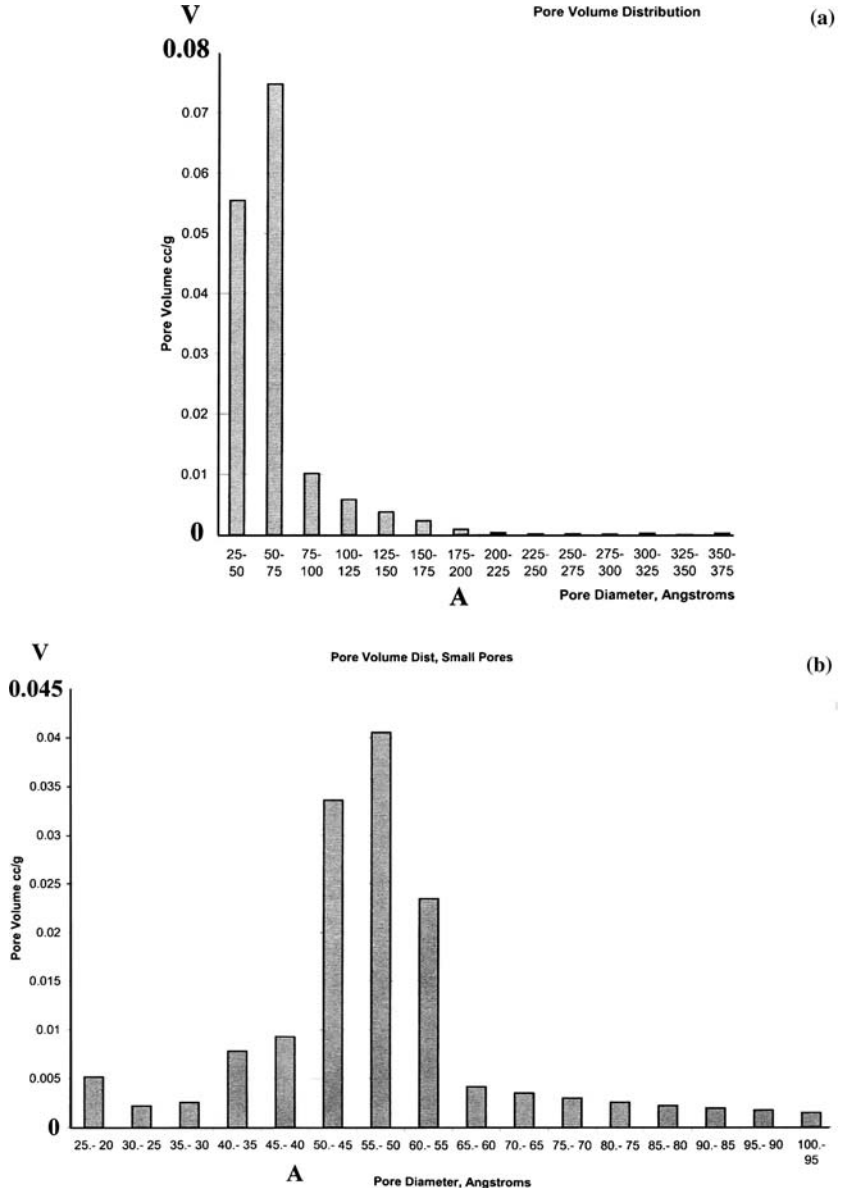

Figure 1. N_2 pore size distribution of ($Co_{0.1}$ $Ru_{0.05}$) nanocatalyst on nanotitania: (a) plot of pore volume (cc/g),V, vs. pore diameter (A) in Angstroms. The horizontal scale extends from 25–50 A to 350–375 A. (b) Enlargement of (a), with average pore diameters of ~5–6 nm. The horizontal scale extends from 25–20 A to 100–95 A.

nanometers were deposited on carbon filmed stainless steel microgrids for *in situ* wet-ETEM. Figure 2a shows dry Co–Ru nanocatalysts on well-ordered rutile in vacuum at room temperature (RT). We carried out real-time monitoring of the dynamic hydrogenation reaction, while the catalyst was immersed in 10 wt% ADN in methanol and 0.75 wt% NaOH solvent, with flowing hydrogen gas, from RT to nominal 100 °C at low vapor pressure of ADN, for different periods. The nucleation of reaction products at the wet catalyst surface was slow between 50 °C and 80 °C, and a rapid growth and clean desorption of reaction products were observed at ~100 °C (figure 2b). Our real-time observations at ~100 °C indicate a highly active and selective catalyst,

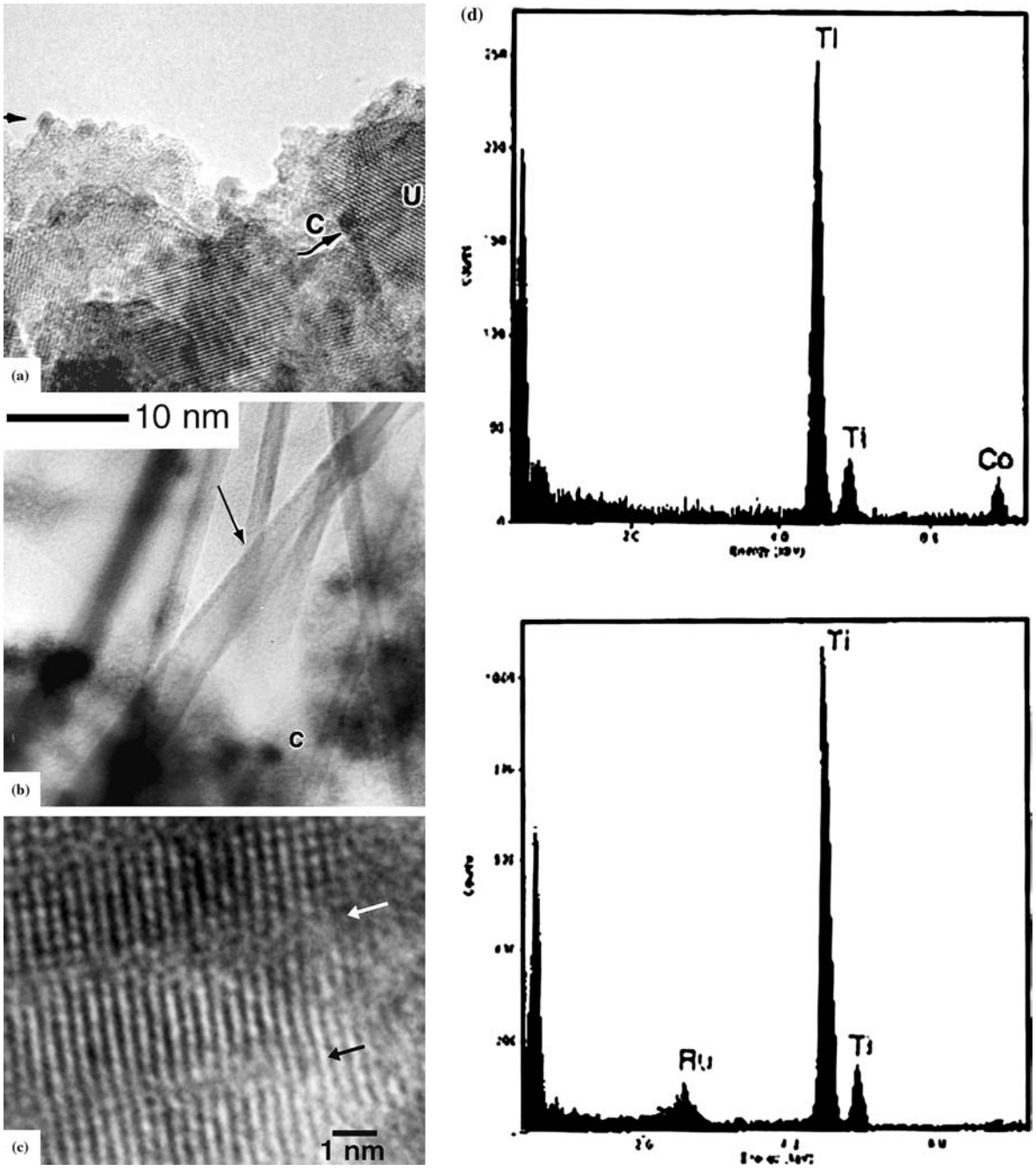

Figure 2. *In situ* imaging of liquid–catalyst–gas reactions. (a) Dry nano Co–Ru/nanotitania in vacuum at RT. The nanocatalysts are indicated by c and arrow, and the well-ordered nanosubstrate lattice, by u. (b) Wet sample: *In situ* hydrogenation of adiponitrile (ADN) in the liquid medium over the catalyst surface at nominal 100 °C showing desorption of nanolayer product (arrowed) (temperature gradient may be present in the liquid). (c) Atomic resolution image of anion vacancy nanodefects in nanotitania (arrowed) dry sample following the hydrogenation. (d) EDX spectra of dry sample for Co (top) and Ru (bottom). Spectra are plotted as counts (arbitrary units) vs. electron energy in keV.

with a growth rate of ~0.25 nm/s. Atomic resolution imaging and analysis after the ADN hydrogenation of the dry sample showed anion vacancy defects in nanotitania following anion loss and crystal glide shear which preserve anion vacancies associated with acid sites [17,21], along ⟨001⟩ direction (figure 2c, arrowed). In the bimetallic system, the growth of the reaction products was found to increase with higher concentration of the defects. We confirmed the formation of the vacancy nanodefects in nanotitania by *in situ* reduction of Co–Ru/TiO_2 in H_2 alone, and alternatively in CO, ruling out hydroxyl formation. The formation of shear defect structures in reduced, anion-deficient titania at > 500 °C has been reported [21,26]. The formation of the defects at the lower temperatures in nanotitania indicates that some anion loss occurs in the presence of the catalysts, resulting in anion vacancies in nanotitania. Atomic imaging and nanoprobe-EDX (figure 2d) showed the particles to be distinct. MS of the desorbed products confirmed the presence of HMD (Figure 3, with peaks at ~117 (HMD + H) at A and 139 (HMD + Na) at B), an important intermediate in the manufacture of the polyamide, nylon 6,6. MS had a resolution of ~630 (calculated by dividing the peak mass by peak width at half height: 117.42 amu/0.186 amu). The data also indicate that the mesoporous systems employed in our studies are capable of providing very high hydrogenation activity.

Simultaneously, *in situ* imaging and MS revealed the evidence for bis-hexamethylene triamine (BHMT; $NH_2(CH_2)_6NH(CH_2)_6NH_2$) on the catalyst surface during the hydrogenation of liquid ADN. BHMT is used in coatings, polyamides, sealants and epoxies. Figure 4a and b show images of the wet nanocatalyst at RT and the desorption of BHMT at ~100 °C, respectively. Figure 4c shows the enlargement of BHMT nanolayers (at H) shown in figure 4b. They

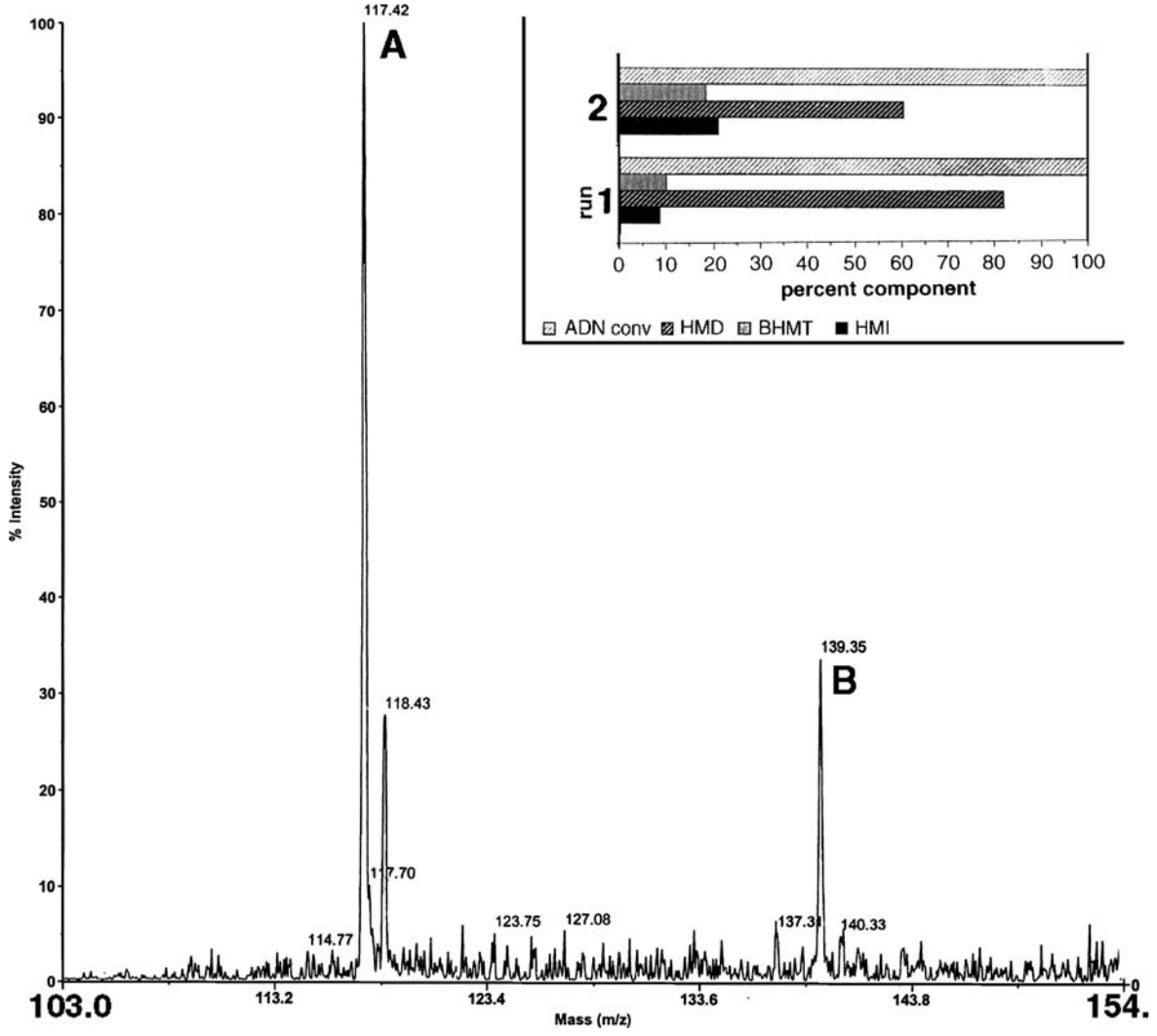

Figure 3. Mass spectrum (MS, % intensity vs. mass (m/z)) of the desorbed product, confirming hexamethylene diamine (HMD) peaks at ~117 (HMD + H) at A and at 139 (HMD + Na) at B. (Inset shows parallel reactivity tests showing very high hydrogenation activity for Co–Ru nanocatalysts over nanotitania (bar 1), compared to unpromoted Ru nanocatalysts (bar 2).

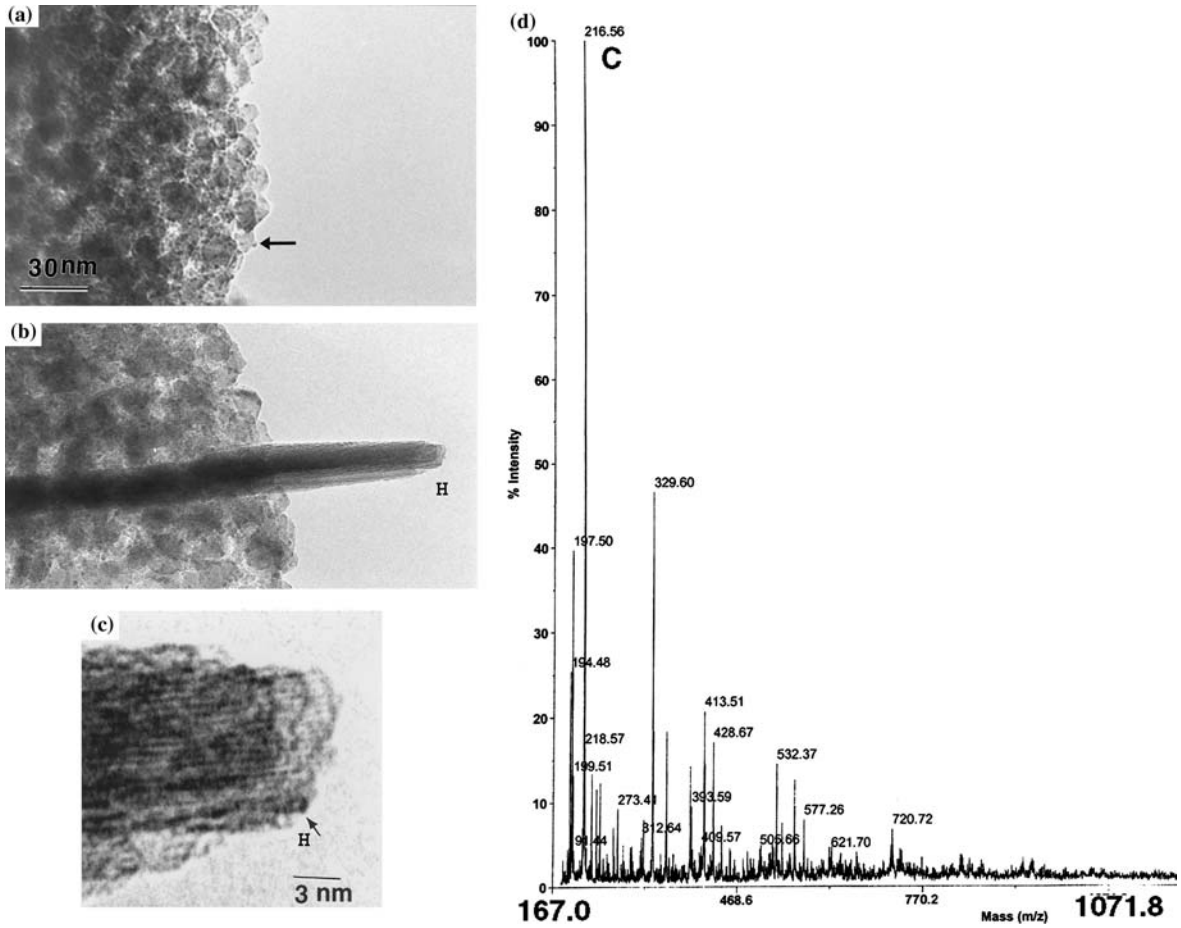

Figure 4. (A) Wet nano Co–Ru/Nanotitania in ADN liquid and H_2 gas at RT. (B) *in situ* growth of BHMT lattice (e.g. at H) at the wet catalyst surface at ~100 °C. (area from (a)). Particles remain stable. (c) Enlargement of wet sample in (b) indicating ~0.56 nm periodicity. (d) MS with protonated BHMT, at C.

indicate the hitherto unknown lattice structure of BHMT with a periodicity of ~0.56 nm. (In *ex situ* studies, upon exposure to air, BHMT can interact with CO_2 and form, e.g. carbamates). MS of the desorbed products confirms the presence of BHMT (figure 4d, with mass peak at C with BHMT + hydrogen at 216.56).

Our studies have shown that the nanocatalysts maintain their structural integrity and elemental form in the reaction environments of H_2 and ADN up to 300 °C, with smooth catalyst recovery. The nanocatalyst particles in figure 2 and figure 4a (e.g. shown by arrow) and b, remain stable, without spreading or sintering on the substrate, confirmed by examining the samples after the reactions. During the hydrogenation, HMD, BHMT and related oligomers formed can sublime and deposit on colder parts of the sample surface under both the pulsed and continuous feed of the ADN liquid. Hexamethylene imine (HMI) is also present. The process with these competing reactions is further complicated by the existence of a temperature gradient in the liquid, the precise nature of it is not known in our experiments. Parallel reactivity tests of Co–Ru/titania catalysts have confirmed the *in situ* ETEM studies of very high hydrogenation selectivity for HMD (up to 85–88%) with the full conversion of ADN (inset in figure 3). Unpromoted Ru catalysts on titania, alumina and other nanosupports (and Au-promoted catalysts) did not show high concentrations of the products [21] and had lower 55–60% selectivity.

We believe that the stability of the catalyst particles on the nanosupports observed in the liquid–catalyst–H_2 gas reactions, is due to surface energy effects. Under equilibrium conditions in liquid and gaseous reaction environments:

$$\gamma_{slg} - \gamma_{ms} = \gamma_{mlg} \cos\theta$$

where γ are surface energies between metal catalyst particles (m), substrate (s), liquid (l) and gas (g) and θ is the contact (wetting) angle between the metal catalyst and the substrate, following Young's well-known equation [27]. In reducing H_2 gas, the surface energy of titania is increased [28]. γ_{mlg} is increased which increases θ values (particles retain their sizes without

spreading on the substrate) and the metal and the substrate interaction is small at the low temperature of the reaction. Consequently, strong metal–substrate interactions (in which, the substrate covers active metal catalyst surface in reducing gases, leading to deactivation), observed at high temperatures of ~500 °C in noble metal/titania [8,9], are absent at the low temperatures (~100 °C) used in our experiments on the nanocatalyst systems, thus prolonging the catalyst life.

We propose the following explanation for the excellent hydrogenation activity observed in the promoted nanocatalysts. In the selective hydrogenation at ~100 °C, partial reduction of the nanotitania support occurs due to the loss of the oxide ion, leading to the formation of anion vacancies and the associated reduced Ti^{3+} species on the surface of the reduced nanotitania. In Ru/titania, the reduction in Ru d-band electron vacancies occurs due to the partial reduction of titania to Ti^{3+} in the reaction environments and electron transfer from the support to Ru rendering it less active for the hydrogenation. On the other hand, in the promoted Co-Ru/titania catalyst, The d-band vacancies of Co are maintained which is key to maintaining the supply of H-atoms necessary for the hydrogenation over Ru. Co is known to activate H. We therefore believe that the combined synergistic effect between the metals and the interaction with the reduced support with anion vacancies (associated with Lewis surface acid sites) resulting in electronic modification, provide highly active sites for the hydrogenation to HMD. The results present guidelines for designing reactive sites for hydrogenation processes in general. The wet-ETEM studies also suggest that there may well be considerable further possibilities in understanding dynamic interactions between organic molecules in a solution phase and inorganic substrates (especially where organic molecular structural integrity may be destroyed upon drying), which may be important in the design of molecular electronics circuitry.

Acknowledgements

We thank L.G. Hanna, P. Peacock, F. Gooding, and S.B. Ziemecki (retired) of DuPont (CRD) for technical assistance and reactivity measurements.

References

[1] C. De Bellefon and P. Fouilloux, Catal. Reviews. Sci. Eng. 36 (1994) 459.
[2] G.J. Kauffman, J. Chem. Ed. 65 (1988) 803.
[3] M. Besson, *et al*., Bull. Soc. Chim. Fr. 127 (1990) 5.
[4] J. Volf *et al*., Stud. Surf. Sci. Catal. 27, L. Cerveny (ed), (Elsevier, 1986) 105.
[5] F. Mares, *et al*., J. Catal. 112 (1988) 145.
[6] H. Greenfield, Ind. Eng. Chem. Prod. Res. Dev. 6 (1967) 142.
[7] T. Nakayama, *et al*., J. Catal. 87 (1984) 108.
[8] S.J. Tauster, *et al*., J. Am. Chem. Soc. 100 (1978) 170.
[9] M.G. Sanchez and J.L. Gasquez, J. Catal. 194 (1987) 120.
[10] P.L. Gai, (Gai-Boyes), Catal. Reviews. Sci. Eng. 34 (1992) 1.
[11] B. Bradley, *Metal Alkoxides* (Academic Press, New York, 1978).
[12] P.L. Gai, K. Kourtakis and S.B. Ziemecki, Micrsc. Microanal. 6 (2000) 335.
[13] P.L. Gai, Micrsc. Microanal. 8 (2002) 335.
[14] Micromeritics Inc., One Micromeritics Drive, Norcross, GA 30093–1877.
[15] S. Brunauer, P.H. Emmett and E. Teller, J. Amer. Chem. Soc. 60 (1938) 309.
[16] E.P. Barret, *et al*., J. Amer. Chem. Soc. 73 (1951) 373.
[17] P.L. Gai, *et al*., Science 267 (1995) 667.
[18] E.D. Boyes and P.L. Gai, Ultramicroscopy 67 (1997) 219.
[19] P.L. Gai, (a) Adv. Mat. 10 (1998) 1259; (b) Top. Catal. 21 (2002) 161.
[20] P.L. Gai, Inst. Phys. Conf. Ser. (London, U.K.), 168- Section 9 (2002) 401.
[21] P.L. Gai and E.D. Boyes, *Electron Microscopy in Heterogeneous Catalysis* (Institute of Physics Publishers, London UK and Philadelphia USA, 2003).
[22] D.F. Parsons *et al*., *Adv. Bio. Med. Phys*., 15, J.H. Lawrence *et al*., (eds) (Acad. Press, New York, 1974), p. 161.
[23] A. Fukami, *et al*., J. Electron Microsc. 34 (1985) 47.
[24] T. Daulton, *et al*., Micrsc. Microanal. 7 (2001) 134.
[25] S. Hanton, Chem. Rev. 3 (2001) 527.
[26] M. Blanchin, *et al*., J. Phys. C3 z(suppl. 6) (1981) 95.
[27] A.M. Stoneham, J. Am. Ceram. Soc. 64 (1981) 54.
[28] E. Ruckenstein, *Growth of metal clusters* J. Bourdon, J. (ed) (Elsevier 1981), 57.